

# PERMANENT MAGNET FLUX-SWITCHING MACHINE, OPTIMAL DESIGN AND PERFORMANCE ANALYSIS

Liviu Emilian SOMESAN<sup>1</sup>, Ioan Adrian VIOREL<sup>1</sup>

<sup>1</sup>Department of Electrical Machines and Drives, Faculty of Electrical Engineering, Technical University of Cluj-Napoca, 28 Memorandumului, 400 114 Cluj-Napoca, Romania

liviu.somesan@emd.utcluj.ro, ioan.adrian.viorel@emd.utcluj.ro

**Abstract.** In this paper an analytical sizing-design procedure for a typical permanent magnet flux-switching machine (PMFSM) with 12 stator and respectively 10 rotor poles is presented. An optimal design, based on Hooke-Jeeves method with the objective functions of maximum torque density, is performed. The results were validated via two dimensions finite element analysis (2D-FEA) applied on the optimized structure. The influence of the permanent magnet (PM) dimensions and type, respectively of the rotor poles' shape on the machine performance were also studied via 2D-FEA.

is developed and an optimization procedure is carried on to obtain the motor with the maximum torque density. The obtained machine structure, dimensions and characteristics were checked via two dimensions finite element analysis (2D-FEA). A suboptimal procedure was carried on to obtain better performance by employing 2D-FEA. The influence on the machine performance of the permanent magnet characteristics (remanent flux density and coercive field intensity) was also analysed by employing 2D-FEA. The conclusions and the final considerations in the case of the sample of PMFSM end the paper.

## Keywords

*Optimal design, performance analysis, PMFSM.*

## 1. Introduction

The permanent magnet flux-switching machine (PMFSM) has a short history and is a relatively new category of electric machines. The basic model of PMFSM was described in [1], where Rauch and Johnson proposed a new type of machine with permanent magnets (PMs) placed in the stator in order to better control their temperature, and was brought back to the scene, in different structures [2], [3], [4], [5], due to its improved performance. PMFSM has been receiving significant attention in the last two decades thanks to the advantages of high power density, mechanical robustness and torque capability [3], [4], [5], [6]. Furthermore, it can be used with success in harsh operating environments, such as aerospace, automotive and wind energy applications [7], [8], [9].

This paper takes into consideration a typical three phase structure of a permanent magnet flux-switching machine with 12 stator poles and 10 rotor poles. For this structure an analytical sizing-designing algorithm

## 2. PMFSM Structure and Dedicated Sizing-Design Algorithm

Figure 1 shows the PMFSM structure. As it can be seen, the rotor of the machine is similar to that of a switched reluctance motor. The number of rotor poles and stator poles differs by two, respectively 10 rotor poles and 12 stator poles. The concentrated windings employed in the PMFSM are similar to those of the switched reluctance motor (SRM). The only difference compared to the SRM consists on the configuration of the stator which contains 12 segments of "U" shape magnetic cores, between which 12 pieces of PMs are inset, the direction of magnetization being reversed from one magnet to the following, as in Fig. 2. The stator winding comprises concentrated coils, each coil being wound around a pole which contains two adjacent laminated segments and a PM. Due to the short end-windings the copper losses have low values. The main designing specifications for the sample PMFSM are:

- Rated output power  $P_{out} = 30$  kW.
- Rated phase voltage  $U_f = 230$  V.
- Rated speed  $n = 3000$  rpm.

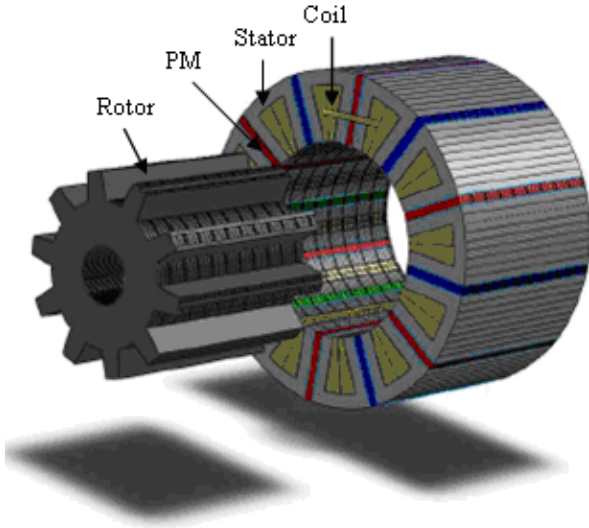


Fig. 1: A 3-phase 12/10 PMFSM, expanded view.

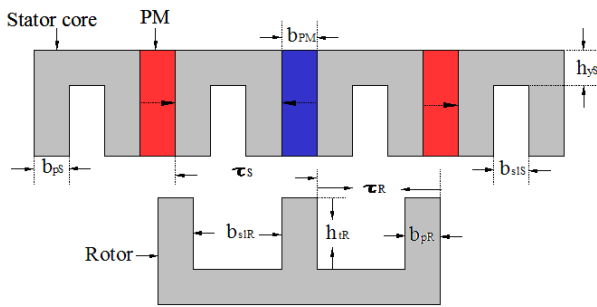


Fig. 2: Cross-section of the PMFSM design.

Figure 2 shows a basic layout of the proposed PMFSM where some of the most important dimensions are evinced.

The PMFSM analytical design is based on an equation which gives the machine air-gap diameter  $D_g$  function of the design specifications, of adopted material properties and of some sizing coefficients  $k_L, k_E$ . The performance related values, efficiency  $\eta$ , power factor  $\cos\varphi$ , maximum air-gap flux density  $B_{gmax}$  and stator electrical loading  $A_s$  must be chosen to consider the existing data, the machine topology and the PM type.

$$D_g = \sqrt[3]{\frac{P_{out} Q_S}{\sqrt{2} \pi^3 Q_R \eta k_L k_E \cos\phi n B_{gmax} A_s}}, \quad (1)$$

where  $Q_S$  and  $Q_R$  are the number of stator and rotor poles,  $k_L$  is the aspect factor (2) and  $k_E$  represents the ratio of the back-*emf* to phase voltage.

The stack length is:

$$l_{st} = k_L D_g. \quad (2)$$

The number of coils turns  $N_t$  is computed with the following equation:

$$N_t = \frac{Q_S E}{\sqrt{2} \pi^2 k_L N_R D_g^2 n B_{gmax}}, \quad (3)$$

where the phase *rms* induced *emf* is:

$$E = N_t 2\pi n \frac{Q_R}{\sqrt{2}} l_{st} \pi \frac{D_g}{Q_S} B_{gmax}. \quad (4)$$

The stator pole dimensions are calculated based on equations (5), (6), (7), the same ratios being valid for the rotor poles by changing  $Q_S$  to  $Q_R$  and, adequately, the pole pitch and pole width factor:

$$\tau_S = \pi \frac{D_g}{Q_S}, \quad (5)$$

$$b_{pS} = k_{pS} \tau_S, \quad (6)$$

$$b_{slS} = \tau_S - b_{pS}, \quad (7)$$

where  $\tau_S$  is the stator pole pitch,  $b_{pS}$  is stator pole width and  $k_{pS}$  is stator pole width factor (6).

In order to improve the torque value and to reduce the cogging torque, a suboptimal procedure was conducted via 2D-FEA. The optimal value of the stator PM width  $b_{PM}$  resulted:

$$b_{PM} = \frac{\tau_S}{5}, \quad (8)$$

The magnetic equivalent circuits were constructed for different situations (aligned and unaligned rotor position) to calculate the no-load main flux, the armature reaction and the most important leakage fluxes [10].

The maximum air-gap density  $\Phi_{max}$  in aligned rotor position is:

$$\phi_{max} = B_{gmax} l_{st} \frac{\pi D_g}{Q_S}. \quad (9)$$

Finally, the electromagnetic torque of the three phase PMFSM can be calculated with:

$$T = \frac{3}{2} Q_R \phi_{max} I_f. \quad (10)$$

The initial peak air-gap flux density was taken  $B_{gmax} = 1,55$  T while the PM of NdFeB type has residual flux density  $B_r = 1,2$  T and coercive field intensity  $HC = 910$  kA/m.

The main dimensions of the PMFSM, calculated using the sizing-design algorithm, are evinced in Tab. 1.

**Tab. 1:** Main geometric dimensions and parameters of PMFSM.

Item	Unit	Value
Number of rotor poles, $Q_R$	-	10
Number of stator poles, $Q_S$	-	12
Machine's outer diameter, $D_{out}$	m	0,277
Shaft diameter, $d_{ax}$	m	0,045
Air-gap diameter, $D_g$	m	0,159
Air-gap length, $g$	m	0,0007
Stator PM width, $b_{PM}$	m	0,008538
Rotor pole pitch, $\tau_R$	m	0,0497
Rotor pole width, $b_{pR}$	m	0,01457
Stator pole pitch, $\tau_S$	m	0,041832
Stator pole width, $b_{pS}$	m	0,011418
Stator slot height, $h_{s1S}$	m	0,04612
Rotor yoke height, $h_{yR}$	m	0,03475
Stack length, $l_{st}$	m	0,159
Stator yoke height, $h_{yS}$	m	0,01249
Number of turns per phase, $N_t$	-	36
Phase current, $I_f$	A	58

Obviously, the sizing procedure may not conduct always to the best results, but it gives quite important information for the designer.

### 3. Design Optimization

An advanced design optimization based on numerical algorithms is applied in order to improve the PMFSM design and the overall system's performances.

In this case, the Hooke-Jeeves method was selected. It is a pattern search method [11], [12], [13] and starts with an exploratory move in which all optimization variables are changed by a predefined step. The pattern move then repeats all changes that were found to be successful in the exploratory move and uses an objective function to evaluate the effect of the combined changes. The main steps in the Hooke-Jeeves algorithm are:

- Choose the optimization variables that will be modified in the optimization process.
- Impose special limitations of other variables that can be altered during the process.
- Define the objective function.
- Set the initial and final value of the global increment. These values will be initially modified with a larger increment, which will be further decreased in order to refine the search space.
- Compute the geometrical dimensions, the magnetic and the electrical values, and evaluate the objective function.
- Make a research movement in the solution space, using the initial step and recomputed the objective function and its gradient.
- Make an optimized variable movement with initial step until the objective function is increasing.
- Repeat the search movement and use the gradient to find the better direction along the new track.
- Reduce the variation increment and repeat the previous steps. The algorithm stops when the search movement cannot find better points even with the smallest increment. The found value represents a local maximum.

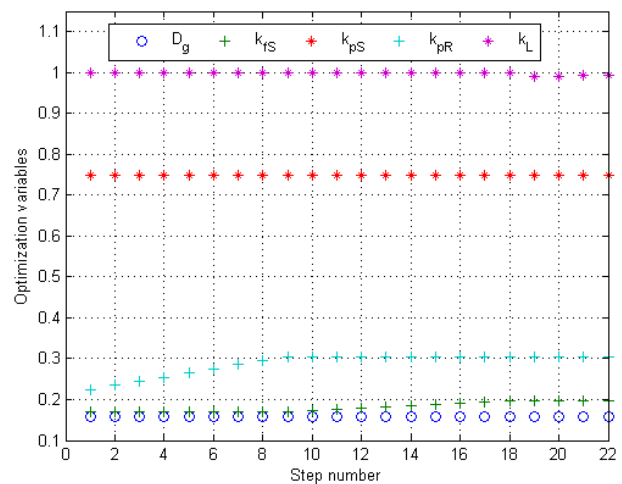
In the case of the proposed PMFSM design, a set of five optimization variables were selected: air-gap diameter,  $D_g$ , stator and rotor pole width factor (6),  $k_{pS}$ ,  $k_{pR}$ , stator pole circumferential length factor,  $k_{fS}$ , and aspect ratio  $k_L$ .

$$k_{fS} = \frac{b_{PM}}{\tau_S}. \quad (11)$$

The next step was to set the minimum and the peak limits for each variable. These limits were set based on the designer experience and it is important to set these adequately.

Finally, the optimization initial and final step sizes are set to 0,001, respectively 0,00001 with an optimization ratio equal with 1,01. The optimization process uses these parameters as increments in the calculation process.

The maximum torque density was considered the objective function for the optimization program. The objective function is represented by the ratio between the torque and the total mass of the PMFSM. In this case, a total number of 22 iterations were necessary. The evolution of the objective function and the main parameters are illustrated in Figs. 3, 4, 5, 6.

**Fig. 3:** Evolution of the optimization variable.

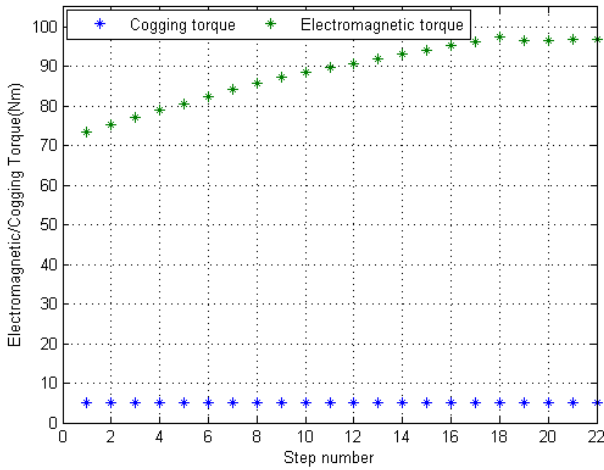


Fig. 4: Evolution of the developed cogging and electromagnetic torque.

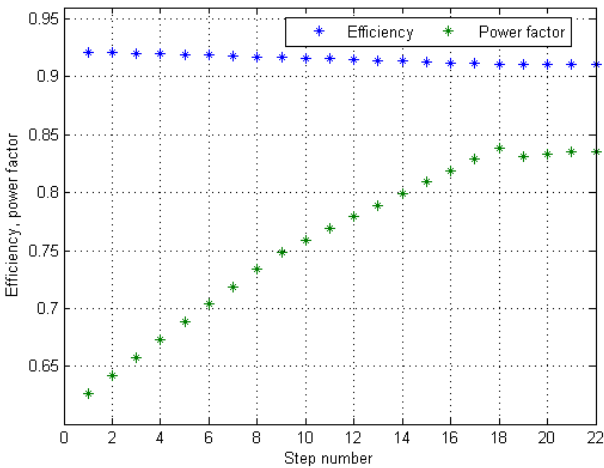


Fig. 5: Evolution of efficiency and power factor.

The evolution of the optimization variables is illustrated in Fig. 3. The air-gap diameter  $D_g$  has reached a value of 0,1587 m, while the aspect factor  $k_L$  has reached the maximum limit of 1. The electromagnetic torque value has been significantly increased from 70 Nm to 99 Nm, Fig. 4. In Fig. 6 it can be seen that the ratio between the torque and PMFSM mass has reached the maximum value of 4,38.

Tab. 2: Optimal PMFSM parameters.

Parameter	Initial value	Optimal value
$D_g$ [m]	0,159	0,159
$b_{pS}$ [m]	0,01041	0,0114
$b_{pR}$ [m]	0,01041	0,0145
$b_{pM}$ [m]	0,01041	0,0084
$k_L$	1	1

The optimal parameters of the improved PMFSM design are given in Tab. 2. In consequence, the op-

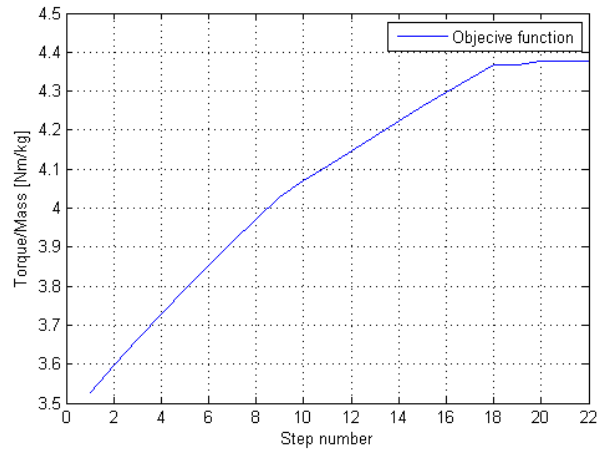


Fig. 6: Evolution of the objective function.

timizing method can be considered a reliable one in reaching its objectives.

## 4. Finite Element Analysis

Two dimensions finite element analysis (2D-FEA), by using the Cedrat FLUX 2D environment, was performed to check the electromagnetic performance of the PMFSM. It was applied on the resulted structure after the maximum torque density optimization process.

The 2D-FEM calculated radial-component of the air-gap flux density is shown in Fig. 7. As it is seen, the maximum air-gap flux density exceeds 2 T and the air-gap field distribution of a PMFSM is far from sinusoidal and exhibits significant harmonics content due to the doubly salient structure.

The 2D-FEA computed static electromagnetic and cogging torque is displayed in Figs. 8 and 9 versus rotor position. The rotor was moved over an electrical period with an increment of 1 mechanical degree, one electrical period corresponding to 36 mechanical degrees. The phase current is the rated one,  $I_f = 58$  A, and the PMs' width is 10,4 mm.

### 4.1. The Influence of PMs Dimensions on the Machine's Performances

The variation of the electromagnetic torque for different dimensions of the PMs is analyzed in this section using 2D-FEA. This aspect is an important one considering the significant contribution of the PMs to the total cost of the machine. Also the variation of the PM dimensions is essential in order to reduce the cogging torque.

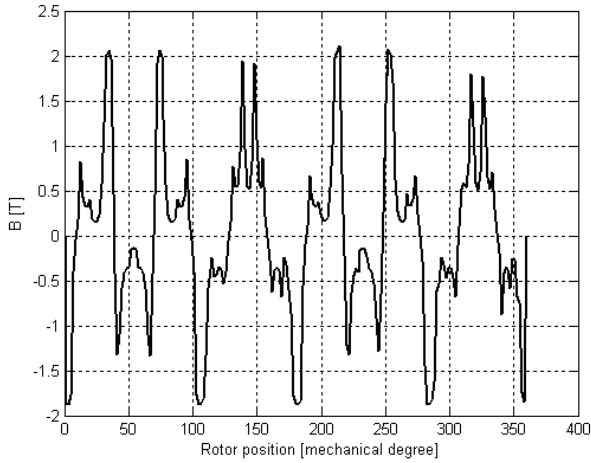


Fig. 7: Air-gap field distribution.

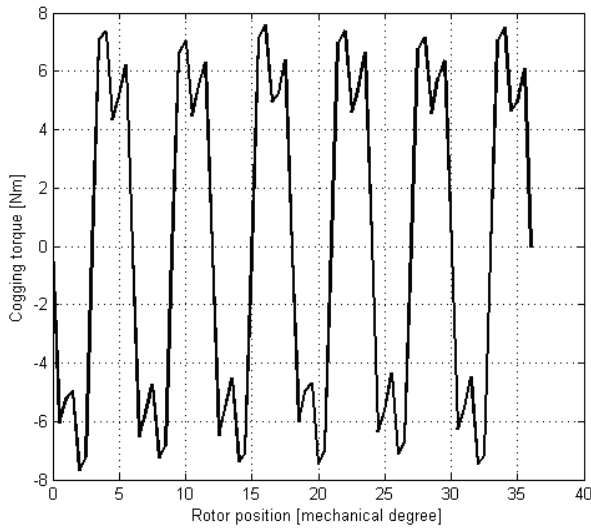


Fig. 8: Cogging torque.

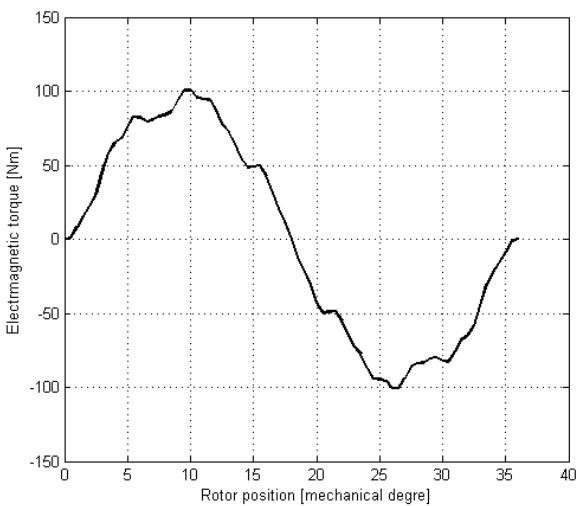


Fig. 9: Electromagnetic torque.

Starting from the initially adopted values, the PM width  $b_{PM}$  was modified from the initial (10,4 mm)

one to the optimized one (48,4 mm). The 2D-FEA computed cogging torque is displayed in Fig. 10.

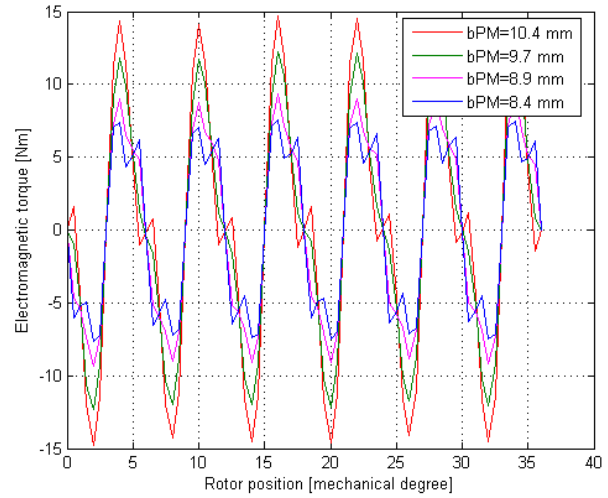


Fig. 10: Evolution of the cogging torque for different values of PMs widths.

The influence of the PM widths on the electromagnetic torque values is not an important one since there are no big changes [14]. Instead, the variation of the cogging torque is an important one. The cogging torque decreases from 14,2 Nm ( $b_{PM} = 10,4$  mm) to 7,36 Nm ( $b_{PM} = 8,4$  mm).

#### 4.2. The Influence of PMs Characteristics on the Machine's Performances

The necessity of a large quantity of PMs and the high price of the permanent magnets used, respectively of NdFeB, made the PMFSM to be more expensive comparatively with the others PM machines.

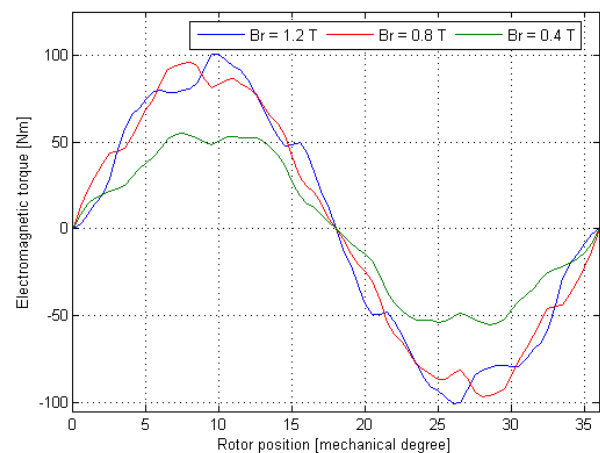


Fig. 11: PMFSM electromagnetic torque for different values of  $B_r$ .

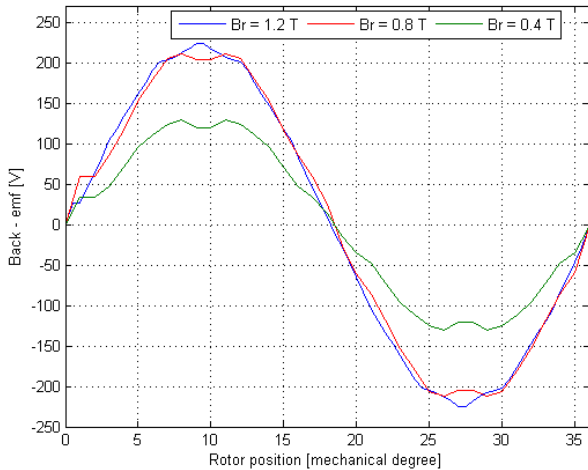


Fig. 12: PMFSM back-emf for different values of  $B_r$ .

The influence of different remanent flux densities values (1,2 T; 0,8 T; 0,4 T) on PMFSM performance is illustrated in Figs. 11 and 12. In all cases the relative permeability is the same.

The variation of electromagnetic torque and back-emf for different values of  $B_r$  and  $H_c$  is illustrated in the above figures. It can be seen from Figs. 11 and 12 that the obtained values for  $B_r = 0,8\text{ T}$  are close to that obtained for  $B_r = 1,2\text{ T}$ . There is a difference of 5 % between the results obtained in the two cases. This difference depends on the ratio of PM's and coil mmf.

### 4.3. The Influence of Rotor Pole Shape on the Cogging Torque

The cogging torque is relative large in the case of PMFSM due to the doubly-salient structure and to the high air-gap flux density produced by PMs. It is usually undesirable because produces vibrations and noise.

Different methods for reducing cogging torque are available in the literature [15]. One of the well-known methods to minimize cogging torque is to modify the shape of the rotor pole. Consequently, the shape of the rotor pole was modified from a rectangular one to a trapezoidal one, as illustrated in Fig. 13. The rotor yoke base width is chosen in this case to be 1,4 times greater than the rotor pole arc.

The evolution of the cogging torque for two different rotor pole shapes at the optimized PM's width ( $b_{PM} = 10,4\text{ mm}$ ) is illustrated in Fig. 14. From the above figure, it can be seen that the cogging torque is reduced with approximately 35 percent, from 7,37 Nm to 4,8 Nm. This value represents approximately 4,75 percent of the developed electromagnetic torque at the rated phase current.

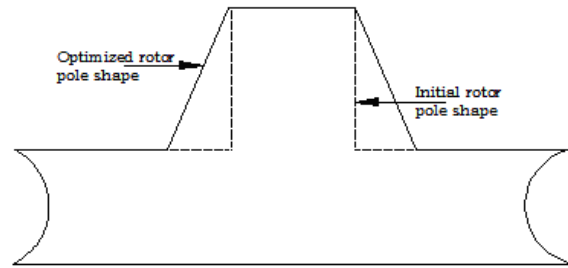


Fig. 13: Rotor pole shape.

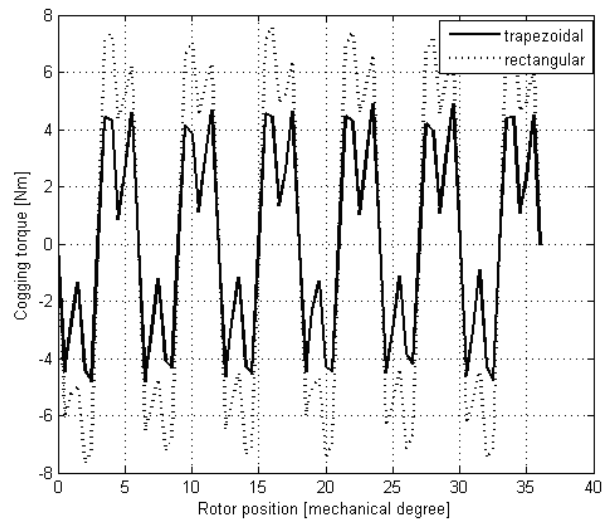


Fig. 14: Cogging torque, different rotor pole shapes.

## 5. Conclusion

In this paper a typical structure of permanent magnet flux-switching machine (PMFSM) with 12 stator poles and 10 rotor poles was proposed. The PMFSM design procedure is based on a specific analytical algorithm.

In order to obtain a machine with improved performance, an optimization procedure based on Hooke-Jeeves method was applied with maximum torque density as the objective function.

2D-FEA analysis was performed to check the electromagnetic performances of the PMFSM. The 2D-FEA was also employed to check the permanent magnet and rotor pole shape influence on the motor's performance. The results in the case of the rotor pole shape influence show that the the cogging torque is reduced with approximately 35 percent when the rotor pole shape is trapezoidal.

A low sensity of the PMFSM torque and back-emf on the permanent magnet qualities for a certain ratio of PM's and coil mmf was proved. It is an important advantage and allows for an essential cost decrease.

## References

- [1] RAUCH, S. E. and L. J. JOHNSON. Design Principles of Flux-Switch Alternators. *Transactions of the American Institute of Electrical Engineers. Part III: Power Apparatus and Systems*. 1955, vol. 74, iss. 3, pp. 1261–1268. ISSN 0097-2460. DOI: 10.1109/AIEEPAS.1955.4499226.
- [2] SARLIOGLU, B., Y. F. ZHAO and T. A. LIPO. A Novel Doubly Saliency Single Phase Permanent Magnet Generator. In: '94, IAS. *Industry Applications Society Annual Meeting*, Piscataway, NJ: IEEE Service Center, 1994, pp. 9–15. ISBN 0-7803-1993-1. DOI: 10.1109/IAS.1994.345505.
- [3] HOANG E., A. H. BEN-AHMED and J. LUCIDARME. Switching Flux Permanent Magnet Polyphased Synchronous Machines. In: *7th European Conference on Power Electronics and Applications*. 1997. vol. 3, pp. 903–908. ISBN 90-75815-02-6.
- [4] BOLDEA, I., C. WANG and S.A. NASAR. Design of a Three-Phase Flux Reversal Machine. *Electric Machines and Power Systems*. August 1999, vol. 27, iss. 8, pp. 849–863. ISSN 0731-356X.
- [5] DEODHAR, R. P., S. ANDERSSON, I. BOLDEA, T. J. E. MILLER. The Flux Reversal Machine: A New Brushless Doubly Salient Permanent Magnet Machine. In: *Conference record/Industry Applications Society, IEEE-IAS Annual Meeting*. San Diego: IEEE, 1996, vol. 2, pp. 786–793. ISBN 0-7803-3544-9. ISSN 0197-2618. DOI: 10.1109/IAS.1996.560174.
- [6] HENNEBERGER, G. and I. A. VIOREL. *Variable Reluctance Electrical Machines*. Aachen: Shaker Verlag, 2001. ISBN 978-3826585685.
- [7] THOMAS, A. S., Z. Q. ZHU, R. L. OWEN, G. W. JEWELL and D. HOWE. Multi-phase Flux-Switching Permanent-Magnet Brushless Machine for Aerospace Application. *IEEE Transactions on Industry Applications*. 2009, vol. 45, iss. 6, pp. 1971–1981. ISSN 0093-9994. DOI: 10.1109/TIA.2009.2031901.
- [8] FANG, Z. X., Y. WANG, J. X. SHEN and Z. W. HUANG. Design and Analysis of a Novel Flux-Switching Permanent Magnet Integrated Starter-Generator. In: *Proceedings of PEMD 2008*. York: IEEE, 2008, pp. 106–110. ISBN 978-0-86341-900-3.
- [9] ZHANG, J., M. CHENG and Z. CHEN. Optimal Design of Stator Interior Permanent Magnet Machine with Minimized Cogging Torque for Wind Power Application. *Energy conversion and management*. 2008, vol. 49, no. 8, pp. 2100–2105. ISSN 0196-8904.
- [10] SOMESAN, L. E., K. HAMEYER, E. PADURARIU, I. A. VIOREL and C. MARTIS. Sizing-Designing Procedure of the Permanent Magnet Flux-Switching Machine Based on a Simplified Analytical Model. In: *13<sup>th</sup> International Conference on Optimization of Electrical and Electronic Equipment OPTIM 2012*. Brasov: IEEE, 2012, pp. 653–658. ISBN 978-1-4673-1650-7. DOI: 10.1109/OPTIM.2012.6231857.
- [11] SOMESAN, L. E., E. PADURARIU, I. A. VIOREL and L. SZABO. Design of a Permanent Magnet Flux-Switching Machine. In: *9<sup>th</sup> International Conference Elektro 2012*. Rajecke Teplice: IEEE, 2012, pp. 256–259. ISBN 978-1-4673-1180-9. DOI: 10.1109/ELEKTRO.2012.6225649.
- [12] RAO, S. S. *Engineering optimization: theory and practice*. 3<sup>rd</sup> Edition. 1996. New York: Wiley. ISBN 04-715-5034-5.
- [13] TUTELEA, L. and I. BOLDEA. Optimal Design of Residential Brushless d.c Permanent Magnet Motors with FEM Validation. In: *International Aegean Conference on Electrical Machines and Power Electronics*. Bodrum: IEEE, 2007, pp. 435–439. ISBN 978-1-4244-0890-0. DOI: 10.1109/ACEMP.2007.4510539.
- [14] SOMESAN, L. E. *A Comparative Study of Permanent Magnet Flux Switching, Permanent Magnet Synchronous and Switched Reluctance Motors, as Possible Solutions in Automotive Drives*. 2012. Ph.D. Thesis. Technical University of Cluj-Napoca, Romania.
- [15] KIM, T. H., S. H. WON, K. BONG and J. LEE. Reduction of cogging torque in flux-reversal machine by rotor teeth pairing. *IEEE Transactions on Magnetics*. 2005, vol. 41, iss. 10, pp. 3964–3966. ISSN 0018-9464. DOI: 10.1109/TMAG.2005.855182.

## About Authors

**Liviu Emilian SOMESAN** was born in Bistrita, Romania, in 1985. He received the B.Sc. and the M.Sc. degree in Electrical Engineering from Technical University of Cluj-Napoca where he obtained his Ph.D. in Electrical Machines in 2012. His research activities are focused on variable reluctance and permanent magnet electric machines.

**Ioan Adrian VIORELE** is Emeritus professor, Department of Electrical Machines and Drives, Technical

University of Cluj-Napoca Romania. He obtained his Ph.D. in Electrical Machines from Politehnica "Traian Vuia" University of Timisoara, Romania in 1978. He published in the field of electric machines more than 200 scientific papers in journals or Conference proceedings and 14 books and tests books, among them a monograph on transverse flux machine. He was visiting

professor or researcher in some Universities or R&D Centers as RWTH Aachen Germany, EPF Lausanne in Switzerland, Ohio State University Akron USA and KERI Changwon Republic of Korea. His major interest is in variable reluctance and permanent magnet electric machine.